

SENTINEL-1 AZIMUTH SUBBANDING FOR MULTIPLE APERTURE INTERFEROMETRY - TEST CASE OVER THE ROI BAUDOIN ICE SHELF, EAST ANTARCTICA

M. Kirkove (1), Q. Glaude (1,2), D. Derauw (1,3), C. Barbier (1), F. Pattyn (2), and A. Orban (1)

(1) Liège Space Center, Université de Liège, Angleur, Belgium

(2) Laboratory of Glaciology, Université Libre de Bruxelles, Bruxelles, Belgium

(3) Instituto de Investigación en Paleobiología y Geología, Universidad Nacional De Rio Negro, General Roca, Argentina

ABSTRACT

As an extension of Synthetic Aperture Radar Interferometry, Multiple Aperture Interferometry (MAI) is a spectral diversity technique that allows the determination of azimuth displacements from phase shift measurements. This is made possible through the creation of backward- and forward-looking Single-Look-Complex (SLC) data. Then, the phase difference between the backward and forward-looking interferogram is translated into a displacement. Using SLC data, MAI requires a proper azimuth splitband operator. Different techniques exist to split the azimuth band, but they are often too briefly described in the MAI literature. In this conference paper, we analyze the signal properties of the Sentinel-1 TOPS acquisition mode and define an azimuth subbanding protocol. In particular, we look at the role of de-apodization and apodization in the band filtering operation. We focus our analysis on Sentinel-1 data in Interferometric Wideswath mode over the Roi Baudouin Ice Shelf, East Antarctica.

Index Terms— Multiple Aperture Interferometry, Splitband, Sentinel-1, Ice Shelf

1. INTRODUCTION

Differential SAR interferometry (InSAR) become a very common tool for measuring displacement maps [1]. The major limitation of InSAR is that it is only sensitive to displacements in one dimension: the light-of-sight direction. This can be overcome using different viewing geometries [2], but this cannot be guaranteed everywhere on Earth, in particular in polar regions.

Multiple Aperture Interferometry (MAI) has been proposed by Bechor and Zebker in 2006 [3], extracting azimuth displacements from a single pair of SAR images. Compared to pixel offset tracking, MAI is estimated to be twice more precise.

This conference paper carefully details the azimuth subbanding approach, required for Multiple Aperture Interferometry. We focus here on the Sentinel-1 data acquired in Interferometric Wide Swath (IW) and Extra Wide (EW) modes

using the Terrain Observation by Progressive Scans (TOPS), but the method is not bounded by the acquisition mode. In section 2, we describe the rationale of the MAI and the implementation of the azimuth subbanding technique. Then, we present spectral results in section 3 and conclude in section 4.

2. METHODS

2.1. Displacements Measurements by MAI

The MAI technique has been proposed to measure along-track displacements [3, 4, 5, 6, 7]. The idea of MAI is to separate the radar echoes emitted by the satellite received when it was behind the target from the echoes received when the satellite was in front of the target, using sub-aperture processing. The technique makes forward- and backward- looking SLC images from SAR raw images by modifying the focusing for simulating two images integrated with a reduced antenna angular beamwidth. The creation of the two forward- and backward-looking SLC images is obtained by modification of the focusing through shifting the Doppler centroids (DCs) and reducing the azimuth bandwidths. Applying InSAR on the forward- and backward-looking SLC images of master and slave data of an InSAR pair produces forward- and backward-looking interferograms. The MAI interferogram is a differential interferogram, created by complex-conjugate multiplication of these two interferograms; the MAI phase is the difference between these forward- and the backward-looking phases.

The MAI phase is proportional to the azimuth displacement. The linear relation is given by :

$$\phi_{MAI} = \frac{2\pi \cdot \Delta x}{L}, \quad (1)$$

L being the length of the antenna and Δx the displacement in resolution unit. Using signal properties, the MAI phase can also be linked to the spectral separation Δf and azimuth sampling frequency ν

$$\phi_{MAI} = \frac{2\pi \cdot \Delta f \cdot \Delta x}{\nu} \quad (2)$$

In many cases, authors are developing MAI from RAW data, by combining the correct echoes to produce the two SAR images. It is also possible to create the subaperture *a posteriori* from SLC images [8]. The forward- and the backward-SLC images can be seen as the products of splitting the initial Doppler spectrum of an SLC image in two subbands of reduced bandwidth having distinct frequency centers.

In this conference paper, we choose to split the Doppler band into two separated subbands with their bandwidth as large as possible. The division in two subbands ensures that the two produced images simulate two different views: the image corresponding to the left subband is the backward-looking SLC image and the other one the forward-looking SLC image [4]. The widths of the subbands are as large as possible to maximize the azimuth resolution, since this latter increases with the azimuth bandwidth. A minimum overlap ensures a large spectral separation and this property implies a high sensitivity to azimuth displacements [8].

2.2. Azimuth subbanding

To provide transitions between the subbands as soft as possible, we split the original azimuth spectrum by multiplying it with two rounded rectangle filters of the same width (fraction of the original full bandwidth) centered on two distinct azimuth frequencies selected symmetrically around the central Doppler centroid (DC) frequency. This operation is called azimuth band splitting. The left filter (F_b) provides the backward-looking SLC image, the right one (F_f) the forward-looking SLC image. The spectral separation is then computed as the distance between the filter centers (C_b and C_f).

To strongly decrease the side lobes of the azimuth signal, an apodization filter F_a is applied at the end of focalization in both azimuth and range directions. Before azimuth band splitting, we must recover the initial azimuth spectrum. To this aim, we apply the inverse of F_a . We call this operation the de-apodization and the filter the de-apodization filter (noted F_{de}).

Executing azimuth band splitting after de-apodization leads to side lobes recovery in the azimuth signal. We perform apodization on each subband after splitting to achieve a correct apodization of the azimuth signal in the forward- and the backward-looking images. We employ apodization filters centered on the center of each subband. These filters are indicated by $F_{a,f}$ and $F_{a,b}$ for the forward- and the backward-looking images, respectively.

The design of the filters F_b and F_f is based on the spectral properties of the azimuth signal of TOPSAR SLC data. Figure 1.a shows the azimuth time-frequency diagram of a single burst. The slope s of the DC frequencies along the azimuth

direction produces azimuth aliasing: although the beam bandwidth (B_D) is smaller than the azimuth sampling frequency (ν), the effective azimuth bandwidth spanned during a burst (B_B) is larger than B_D , so that the sampling criterion for ν (i.e., $B_B > \nu$) is not fulfilled.

To circumvent the azimuth aliasing problem, we apply azimuth band splitting on data obtained after deramping, a process consisting in removing the slope of the DC frequencies. This operation is equivalent to the frequency scaling technique applied in the CSL TOPSAR processor [9]. Figure 1.b shows what becomes the azimuth time-frequency diagram of a single burst after deramping.

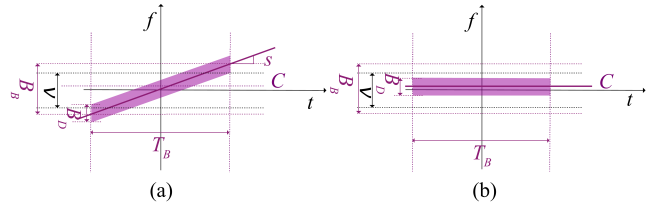


Fig. 1. Azimuth time-frequency diagram of a single burst (a) acquired in TOPS, (b) after deramping. f represents the Doppler frequency, t the azimuth time, T_B the burst time, ν the azimuth sampling frequency, B_D the azimuth bandwidth of a beam, B_B the full Doppler bandwidth, C the center of DC frequencies of the burst and s the DC rate.

The characteristics of the azimuth spectrum (C and B_B) depend on the slant range coordinates. Figure 2.a represents the Doppler spectrum of an azimuth line of a single burst after deramping. In this figure, the notation B_B is replaced by B . The application of azimuth band splitting to this spectrum is illustrated in Figure 2.b where the two filters F_b and F_f are displayed in light and dark blue. Their bandwidth is indicated by B_s .

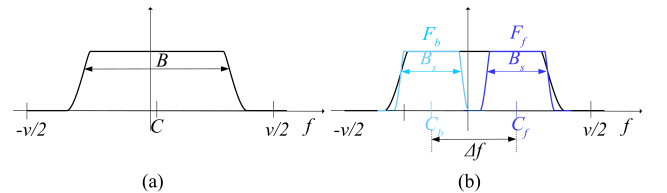


Fig. 2. (a) Doppler spectrum of an azimuth line of a single burst of SLC data after deramping, (b) azimuth band splitting (the two filters are displayed in dark and light blue).

The spectral separation Δf is the distance between the centres in the frequency space:

$$\Delta f = 2C_f - 2C \quad (3)$$

Figure 3 shows the block-diagram of azimuth subbanding applied to a single burst. For Sentinel-1 format, the main

input data are a SLC image (resulting of deramping applied after acquisition) and a metadata file (an XML file containing the metadata of the sub-swath including the burst). The outputs are the burst of the forward- and the backward-looking SLC images. Initialization consists in (1) extracting the burst data from the input data, (2) estimating the range-dependent parameters C from the data and (3) setting the filters F_{de} , F_f , F_b , $F_{a,f}$, $F_{a,b}$. After initialization, the core of azimuth subbanding (azimuth band splitting) is executed. First, the processes of (1) azimuth fast Fourier transform (FFT), (2) de-apodization (multiplication by F_{de}), and (3) azimuth band splitting (multiplication by F_b and F_f) are carried out to provide two products (corresponding to the forward- and the backward-looking SLC images). Then, the processes of (4) apodization (multiplication by $F_{a,b}$ or $F_{a,f}$) and (5) azimuth inverse fast Fourier transform (IFFT) are applied to each product for finally providing the burst of the forward- and the backward-looking SLC images.

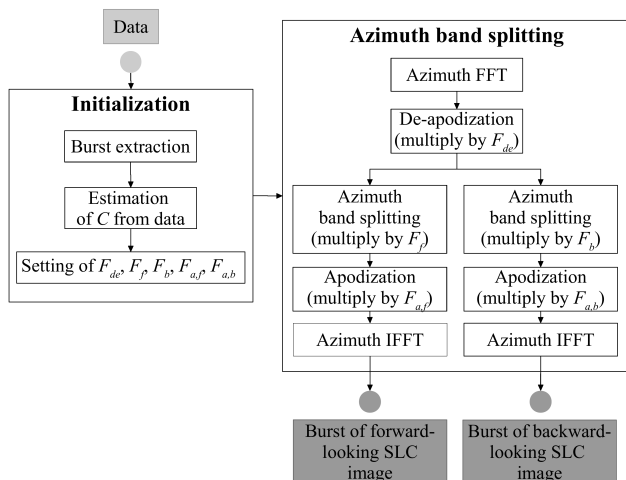


Fig. 3. Block-diagram of azimuth subbanding applied to a single burst. Inputs are shown in light grey, outputs in dark grey.

3. DATA AND RESULTS

In this work, we consider Sentinel-1 SLC images in EW mode, on relative orbit 88, over the Roi Baudouin Ice Shelf (East Antarctica). Acquisition dates are the 20 and 26th of October 2018.

Figure 4 summarizes the spectral results of the subbanding approach. First, the Sentinel-1 data are deramped and the azimuth spectrum is computed (Figure 4.a). From there, the bandwidth and center of the azimuth spectrum of SLC data are derived. At mid-range, these are evaluated at 233 and -8.12343 Hz, respectively. These parameters are required for the definition of the bandpass filters (Figure 4.c, in red).

Then, the de-apodization filter is applied to enhance the signal by reducing side lobes (Figure 4.b). Figure 4.c shows the bandpass filtered signals, with their respective filter. The left and right filters correspond to the backward- and forward-looking Single-Look-Complex data. In Figure 4.d, the results after the apodization are displayed. In the end, the signal is split into two subbanded signals, focused around different Doppler frequencies.

4. CONCLUSION

In this conference paper, we carefully described one approach to split the azimuth band for Multiple Aperture Interferometry (MAI). Particular attention was drawn to the Sentinel-1 TOPSAR acquisition mode. First, the azimuth spectrum of deramped Sentinel-1 acquisition was analyzed, allowing to extract the different parameters of the bandpass filter. We employed a de-apodization filter to decrease the sidelobes of the signal. Then, the signal is split using two rounded rectangle filters. Finally, an apodization filter is applied to recover the original signal properties. The approach was applied on Sentinel-1 acquisitions in Interferometric Wideswath mode, on the Roi Baudouin Ice Shelf, Antarctica. The results show the ability of the technique in providing azimuth band splitting of the data. In future work, the exploitation of these results from Multiple Aperture Interferometry will be discussed.

5. ACKNOWLEDGMENTS

This research is supported by the French community of Belgium in the funding context of a FRIA grant, and carried out in the framework of the MIMO (Monitoring melt where Ice Meets Ocean) and SMAIAD (Sentinel-1 Multiple Aperture Interferometry for Azimuth Displacement Retrieval) projects funded by the Belgian Science Policy contracts Nos. SR/00/336 and Nos. SR/12/207.

6. REFERENCES

- [1] Didier Massonnet, Marc Rossi, César Carmona, Frédéric Adragna, Gilles Peltzer, Kurt Feigl, and Thierry Rabaute, “The displacement field of the Landers earthquake mapped by radar interferometry,” *Nature*, vol. 364, no. 6433, pp. 138–142, 1993.
- [2] Tim J. Wright, Barry E. Parsons, and Zhong Lu, “Toward mapping surface deformation in three dimensions using insar,” *Geophysical Research Letters*, vol. 31, no. 1, 2004.
- [3] Noa B.D. Bechor and Howard A. Zebker, “Measuring two-dimensional movements using a single InSAR pair,” *Geophysical Research Letters*, vol. 33, no. 16, pp. 1–5, 2006.

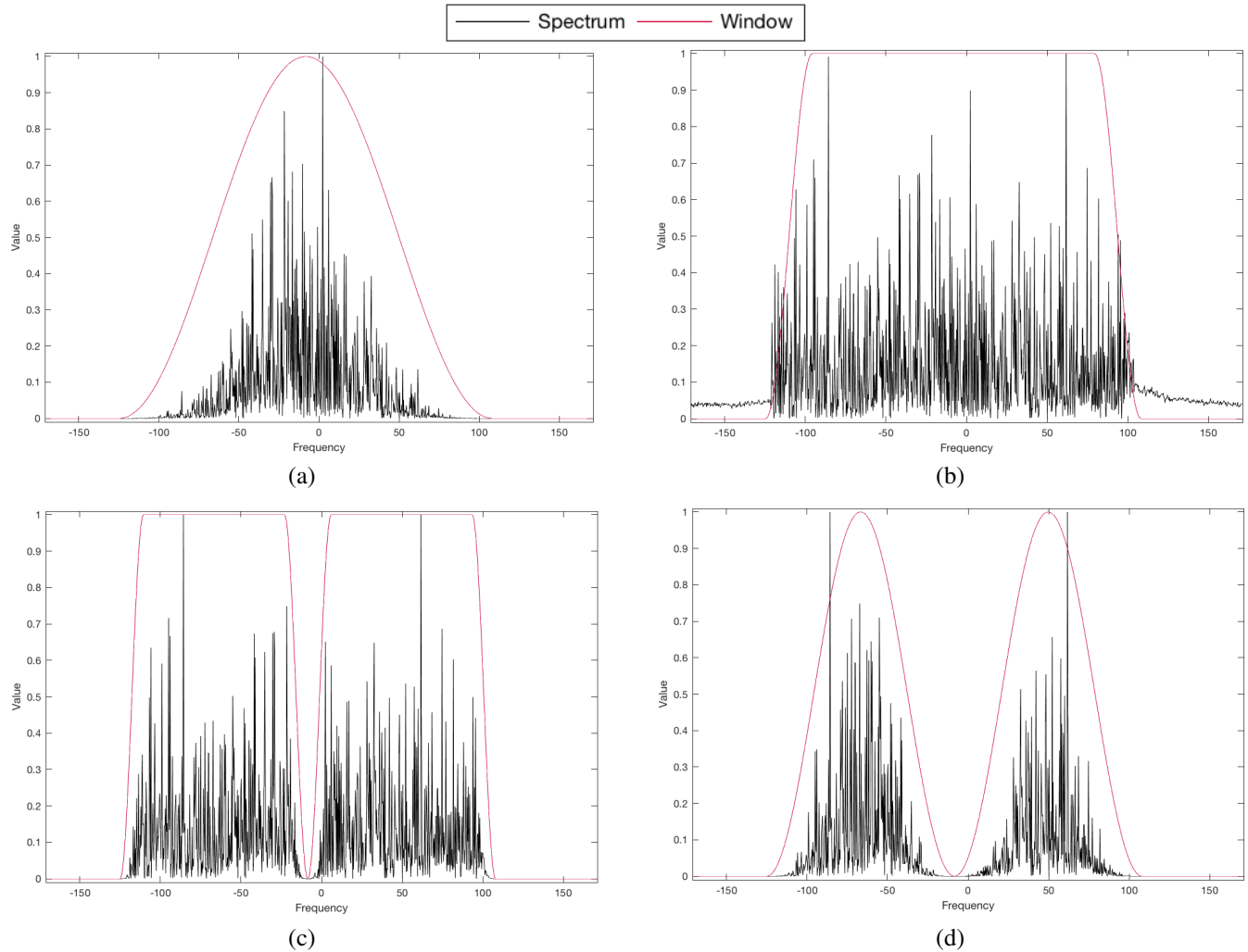


Fig. 4. Spectrum of azimuth line at mid-range ((a) initial, (b) after de-apodization, (c) after band splitting, (d) after apodization). In (c) and (d), both split signals are displayed; the left and right corresponding to the backward- and forward-looking parts of the signal, respectively.

- [4] Hyung Sup Jung, Joong Sun Won, and Sang Wan Kim, “An improvement of the performance of multiple-aperture SAR interferometry (MAI),” *IEEE Transactions on Geoscience and Remote Sensing*, vol. 47, no. 8, pp. 2859–2869, 2009.
- [5] H. Jung, Z. Lu, and L. Zhang, “Feasibility of along-track displacement measurement from sentinel-1 interferometric wide-swath mode,” *IEEE Transactions on Geoscience and Remote Sensing*, vol. 51, no. 1, pp. 573–578, 2013.
- [6] Hyung Sup Jung, Won Jin Lee, and Lei Zhang, “Theoretical accuracy of along-track displacement measurements from multiple-aperture interferometry (MAI),” *Sensors (Switzerland)*, vol. 14, no. 9, pp. 17703–17724, 2014.
- [7] Pietro Mastro, Carmine Serio, Guido Masiello, and Antonio Pepe, “The multiple aperture sar interferometry (mai) technique for the detection of large ground displacement dynamics: An overview,” *Remote Sensing*, vol. 12, no. 7, 2020.
- [8] H J Jiang, Y Y Pei, and J Li, “Sentinel-1 TOPS interferometry for along-track displacement measurement,” *IOP Conference Series: Earth and Environmental Science*, vol. 57, pp. 012019, feb 2017.
- [9] M. Kirkove, A. Orban, D. Derauw, and C. Barbier, “A topsar processor based on the omega-k algorithm: Evaluation with sentinel-1 data,” in *Proceedings of EUSAR 2016: 11th European Conference on Synthetic Aperture Radar*, 2016, pp. 1–5.